Effect of MoO3 on electron paramagnetic resonance spectra, optical spectra and dc conductivity of vanadyl ion doped alkali molybdo-borate glasses

ARTICLE *in* JOURNAL OF MOLECULAR STRUCTURE · DECEMBER 2013

Impact Factor: 1.6 · DOI: 10.1016/j.molstruc.2013.12.041

5 AUTHORS, INCLUDING:

Satish Khasa

Deenbandhu Chhotu Ram University of Sci…

45 PUBLICATIONS **249** CITATIONS

SEE PROFILE

M. Arora

National Physical Laboratory - India

15 PUBLICATIONS **89** CITATIONS

SEE PROFILE

Journal of Molecular Structure 1060 (2014) 182–190

Contents lists available at ScienceDirect

Journal of Molecular Structure

journal homepage: www.elsevier.com/locate/molstruc

Effect of MoO_3 on electron paramagnetic resonance spectra, optical spectra and dc conductivity of vanadyl ion doped alkali molybdo-borate glasses

A. Agarwal [a], S. Khasa [b,*], V.P. Seth [c], S. Sanghi [a], M. Arora [d]

[a] Department of Applied Physics, Guru Jambheshwar University of Science and Technology, Hisar 125001, Haryana, India
[b] Department of Physics, Deenbandhu Chhotu Ram University of Science and Technology, Murthal, Sonipat 131093, Haryana, India
[c] Department of Physics, P.D.M Engineering College, Bahadurgarh 124001, India
[d] EPR Section, National Physical Laboratory, New Delhi 110012, India

ARTICLE INFO

Article history:
Received 14 August 2013
Received in revised form 7 December 2013
Accepted 9 December 2013
Available online 21 December 2013

Keywords:
EPR
Vanadyl ion
Borate glasses
Ionic conduction
Optical properties

ABSTRACT

Alkali molybdo-borate glasses having composition $xMoO_3\cdot(30-x)M_2O\cdot70B_2O_3$ and $xMoO_3\cdot(70-x)B_2O_3\cdot30M_2O$ (M = Li, Na, K) with $0 \leqslant x \leqslant 15$ (mol%) doped with 2.0 mol% of V_2O_5 have been prepared in order to study the influence of MoO_3 on electrical conductivity, electron paramagnetic resonance (EPR) and optical spectra. From EPR studies it is observed that V^{4+} ions in these samples exist as VO^{2+} ions in octahedral coordination with a tetragonal compression and belong to C_{4v} symmetry. The tetragonal nature and octahedral symmetry of $V_{4+}O_6$ complex increase as well as decrease depending upon the composition of glasses with increase in MoO_3 but $3d_{xy}$ orbit of unpaired electron in the VO^{2+} ion expands in all the glasses. The decrease in optical band gap suggests that there is an increase in the concentration of non-bridging oxygen's. From the study of optical transmission spectra it is observed that for all the glasses the degree of covalency of the σ-bonding decreases with increase in MoO_3 content and the degree of covalency of the π-bonding also varies. These results based on optical spectroscopy are in agreement with EPR findings. It is found that dc conductivity decreases and activation energy increases with increase in MoO_3:M_2O (M = Li, Na, K) ratio in $MoO_3\cdot M_2O\cdot B_2O_3$ glasses, whereas the conductivity increases and activation energy decreases with increase in MoO_3:B_2O_3 ratio in $xMoO_3\cdot B_2O_3\cdot M_2O$ glasses, which is governed by the increase in nonbridging oxygen's. The variation in theoretical optical basicity, Λth is also studied.

1. Introduction

Recently many authors [1–10] devoted their work towards molybdenum doped oxide glasses but few of them [5–10] studied the effect of molybdenum ion on EPR, electrical and optical properties of mixed transition metal doped alkali borate glasses. In alkali oxide glasses the electrical conductivity depends on the mobility and concentration of mobile alkali ions. On the other hand, the oxide glasses containing transition metal ions exhibit a purely electronic conductivity with a polaronic conduction mechanism. The conduction process proceeds via a charge exchange among the transition metal ions of different valence states, owing to the loss of oxygens during the formation of the glasses and to the associated reduction of transition metal cation [11–13]. A glass based on a mixture of both transition and alkali metals exhibits a mixed ionic and electronic conductivity [14,15]. Electron paramagnetic resonance (EPR) spectroscopy can be used to study the microstructure around the transition metal ions in glasses [16–21]. The optical band gap studies of oxide glasses provide information related to their electronic structure [22–27]. Molybdenum containing glasses possess a variety of specific features, which arouse interest in view of their applications. It is known that MoO_3 adds to glass semiconductor properties with n-type conduction because of different valence states of molybdenum [28]. MoO_3 containing glasses are also used for the development of optical and radiation glasses [4,29]. In the present paper alkali molybdo-borate glasses doped with 2.0 mol% of V_2O_5 have been prepared in order to study the influence of MoO_3 on the EPR, optical spectra and electrical conductivity.

The compositions of the glass systems studied are given below:

(i) $xMoO_3\cdot(30-x)M_2O\cdot70B_2O_3$ (M = Li, Na and K): MB series
(ii) $xMoO_3\cdot(70-x)B_2O_3\cdot30M_2O$ (M = Li, Na and K): BM series with $0 \leqslant x \leqslant 15$ (mol%).

* Corresponding author. Tel.: +91 130 2484136; fax: +91 130 2484003.
E-mail address: skhasa@yahoo.com (S. Khasa).

0022-2860/$ - see front matter © 2013 Elsevier B.V. All rights reserved.
http://dx.doi.org/10.1016/j.molstruc.2013.12.041

2. Experimental

2.1. Glass preparation

The glass samples were prepared using melt-quench technique from analytical reagent grade chemicals (Himedia, India) M_2CO_3 (M = Li, Na, K), MoO_3, H_3BO_3 and V_2O_5. The chemicals were thoroughly mixed in the required proportions and were melted in crucibles using an electric muffle furnace with normal atmosphere for 30 min at 1373 K. To assure homogeneity, the melt was swirled frequently. The homogenized melt was poured onto a carbon plate and quickly pressed with another.

2.2. EPR measurements

The first derivative EPR spectra were recorded at the room temperature in the X-band ($\nu \sim 9.3$ GHz) on EPR spectrometer (Varian E-109). The magnetic field was modulated by 100 KHz. Polycrystalline DPPH was used as the standard g maker ($g \sim 2.0036$) for the calculation of the spin Hamiltonian parameters.

2.3. Optical spectra

The optical transmission and absorption spectra of the samples were recorded at room temperature using Perkin Elmer UV/Vis spectrometer (Lambda 20) in the wavelength range 350–850 nm.

2.4. dc conductivity

To measure dc conductivity, sample in the form of slice of nearly one-mm uniform thickness were ground to obtain parallel surfaces. The parallel surfaces of the samples were coated with colloidal silver paint as an electrode material. Conductivity measurements were made by the two terminal methods over a temperature range from about 373 K to 593 K. A constant voltage of 10 V was applied across the sample and the circulating current was measured by using a Keithley 6517 programmable electrometer/source.

3. Results

3.1. EPR

Figs. 1 and 2 show the EPR spectra of the VO^{2+} ions in xMoO$_3$·$(30-x)$Li$_2$O·70B$_2$O$_3$ and xMoO$_3$·$(70-x)$B$_2$O$_3$·30Li$_2$O glass samples. These spectra show structure which is due to a hyperfine interaction of a single unpaired electron with a ^{51}V nucleus whose nuclear spin (I) is 7/2. Similar EPR spectra were obtained for other glass samples. These spectra were analyzed by assuming [17–19] that vanadium is present as a vanadyl ion in a ligand field of C_{4V} symmetry. The spin Hamiltonian used is of the form as described by equation given by Hecht et al. [14]. The solutions of the spin Hamiltonian equation are given by suggested by Bleaney [15] for the parallel and perpendicular orientations, respectively.

The calculated value of Spin Hamiltonian parameters (SHP) of the VO^{2+} ion for the EPR spectra for all the glasses are presented in Tables 1 and 2. The uncertainty in the value of g is ±0.0010 and in the value of A is $\pm 1.0 \times 10^{-4}$ cm^{-1} satisfying the calculated value of line position with the corresponding experimental value. The dipolar hyperfine coupling parameter, $P = 2\gamma\beta\beta_N < r^{-3} >$, and the Fermi contact interaction term, K, are evaluated using the equations developed by Kivelson et al. [30].

K is found to be positive for transition metal ions [31]. From the molecular orbital theory, it can also be shown [32] that the compo-

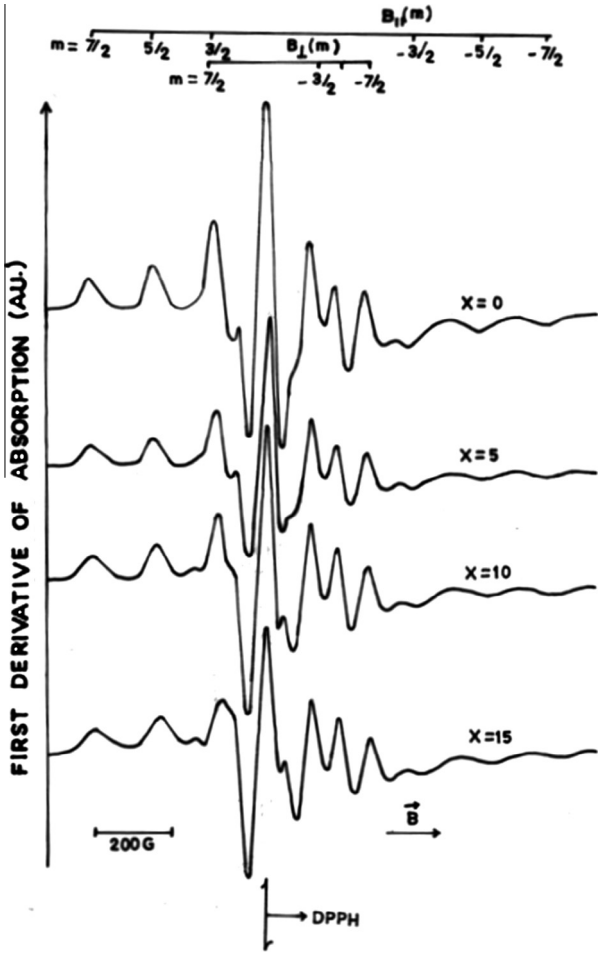

Fig. 1. The EPR spectra of xMoO$_3$·$(30-x)$Li$_2$O·70B$_2$O$_3$ glasses doped with 2 mol% of V_2O_5 in the X-band at 300 K.

nents $A_{\|}$ and $A_{\perp}$ consist of the contributions $A'_{\|}$ and $A'_{\perp}$ of the $3d_{xy}$ electron to the hyperfine structure and the PK term arises due to the anomalous contribution of the s-electrons. The values of $A'_{\|}$, $A'_{\perp}$ and $\Delta g_{\|}/\Delta g_{\perp}$, which measures the tetragonality of the vanadium site [32], are included in Tables 3 and 4. For vanadyl ion an octahedral site symmetry [14] with tetragonal compression would give $g_{\|} < g_{\perp} < g_e$ and $|A_{\|}| > |A_{\perp}|$, the values of SHP obtained in the present study satisfy these observations. Thus, it may be concluded that V^{4+} ions in the present glasses exist as VO^{2+} ions in octahedral coordination with a tetragonal compression and belong to C_{4V} symmetry.

Theoretical optical basicity, Λth, has also been calculated and its calculated values are given in Tables 1 and 2.

3.2. Optical spectra

Figs. 3 and 4 show the optical transmission spectra of xMoO$_3$·$(30-x)$Na$_2$O·70B$_2$O$_3$ and xMoO$_3$·$(70-x)$B$_2$O$_3$·30Na$_2$O glass samples. Figs. 5 and 6 show the optical absorption spectra of xMoO$_3$·$(30-x)$Li$_2$O·70B$_2$O$_3$ and xMoO$_3$·$(70-x)$B$_2$O$_3$·30Li$_2$O glass samples. Similar spectra were obtained for other glass samples. From these spectra, it is observed that the optical absorption edges are not sharply defined which is a characteristic of amorphous material. The values of the cutoff wavelength (λ_{cutoff}) are shown in Tables 5 and 6 for all the samples. The absorption coefficient, $\alpha(\nu)$ was determined from the absorption spectra and Tauc's plots for xMoO$_3$·$(30-x)$Li$_2$O·70B$_2$O$_3$ and xMoO$_3$·$(70-x)$B$_2$O$_3$·30Li$_2$O glass

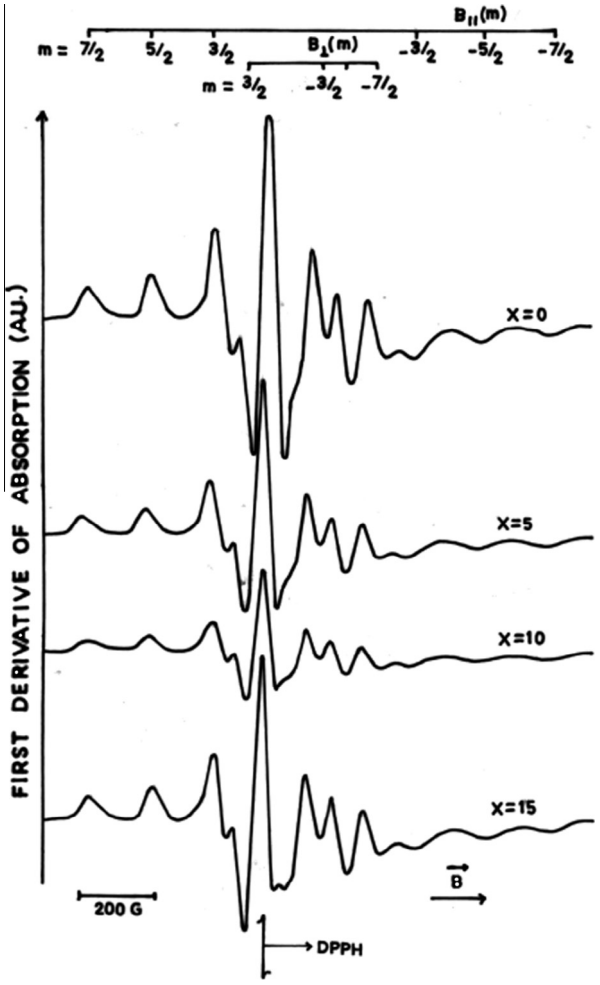

Fig. 2. The EPR spectra of $x MoO_3 \cdot (70 - x)B_2O_3 \cdot 30Li_2O$ glasses doped with 2 mol% of V_2O_5 in the X-band at 300 K.

samples are shown in Figs. 7 and 8. The optical band gap, E_g and band tailing parameter, B have been determined from these plots and their values are shown in Tables 5 and 6. The values of the Urbach's energy, ΔE were calculated from the slopes of the linear region of the curves, $\ln\alpha$ versus $h\nu$, and by taking their reciprocals. The values of ΔE are also included in these tables.

3.3. dc conductivity

Figs. 9 and 10 show the temperature dependence of the dc conductivity for $x MoO_3 \cdot (30 - x)Li_2O \cdot 70B_2O_3$ and $x MoO_3 \cdot (70 - x)B_2O_3 \cdot 30Li_2O$ glass samples, respectively. In these figures the plots of Log σ versus reciprocal of temperature has been shown for the temperature range in which there is a linear relationship between these two parameters. This linear relationship indicates that the temperature dependence of the dc conductivity obeys the well-known Arrhenius law. Similar variation of conductivity was observed for other glasses. The values of activation energy *W*, $\mathrm{Log}\,\sigma_0$, and σ at two extremes of the temperature are shown in Tables 7 and 8. The variation of W with the mol% of MoO_3 in all the glass systems is shown in Figs. 11 and 12. It is observed from Fig. 7 and Tables 7, that the dc conductivity decreases and the activation energy, W increases with increase in MoO_3:M_2O (M = Li, Na and K) ratio keeping B_2O_3 constant. Similarly from Fig. 8 and Tables 8 it is observed that, with increase in MoO_3:B_2O_3 ratio at constant M_2O, dc conductivity increases whereas activation energy decreases.

4. Discussion

4.1. EPR

4.1.1. $xMoO_3 \cdot (30 - x)M_2O \cdot 70B_2O_3$ and $xMoO_3 \cdot (70 - x)B_2O_3 \cdot 30M_2O$ (M = Li, Na and K) glasses

From Tables 1–4 it is observed that the values of $g_{\|}$, $|A_{\|}|$, *P*, $|A'_{\|}|$ and $|A'_{\perp}|$ decrease whereas the values of K and $\Delta g_{\|}/\Delta g_{\perp}$ increase with increase in the MoO_3 content. The values of $g_{\perp}$ and $|A_{\perp}|$ increase with increase in MoO_3 content in MB series whereas in BM series the variation in the values of $g_{\perp}$ and $|A_{\perp}|$ is within experimental error. As suggested by Kivelson et al. [30], we assume that the increase in the value of K with increase in MoO_3 content is due [33–35] to an increase in the tetragonal nature of the $V^{4+}O_6$ complex because of a strongly bonded oxygen at the V^{4+} ion in the site opposite to the vanadyl oxygen. The increase in $\Delta g_{\|}/\Delta g_{\perp}$ also shows that the octahedral symmetry is reduced with increase in MoO_3 content. The decrease of the anisotropic contribution (i.e., $|A'_{\|}|$and$|A'_{\perp}|$) of the $3d_{xy}$ electron to the hyperfine splitting is brought about by increasing [32] screening of the $3d_{xy}$ orbital from its nucleus through overlap of the electron orbits of the surrounding oxygen ligands. This screening produces an expansion of the $3d_{xy}$ orbital, resulting in a decreased interaction between this electron with the vanadium nucleus. Decrease in the value of *P* also supports the argument that the $3d_{xy}$ orbit expands with increase in mol% of MoO_3 in both the series.

Theoretical optical basicity serves in the first approximation as a measure [36] of the ability of oxygen to donate a negative charge in the glasses. In other words, the optical basicity reflects the Lewis basicity of the oxide glasses. As the ability of the equatorial ligands to donate the electron (i.e., Lewis basicity) decreases, σ bonding between V^{4+} and the ligands reduces [37]. This reduction, in turn,

Table 1
Spin Hamiltonian parameters[a] of VO^{2+} at room temperature and Λth in $x MoO_3 \cdot (30 - x)M_2O \cdot 70B_2O_3$ (M = Li, Na & K) glasses.

Glass no.	*x* (mol%)	V_2O_5 (mol%)	$g_{\|}$ (±0.0010)	$g_{\perp}$ (±0.0010)	$\lvert A_{\|}\rvert$ (10^{-4} cm^{-1}) (±1.0)	$\lvert A_{\perp}\rvert$ (10^{-4} cm^{-1}) (±1.0)	Λth
LB1	0	2	1.9374	1.9720	162.8	58.9	0.4940
LB2	5	2	1.9345	1.9711	162.6	58.9	0.4830
LB3	10	2	1.9308	1.9770	161.4	62.8	0.4728
LB4	15	2	1.9294	1.9776	160.3	64.2	0.4635
NB1	0	2	1.9391	1.9711	160.2	57.1	0.5134
NB2	5	2	1.9362	1.9711	160.0	58.9	0.4985
NB3	10	2	1.9322	1.9750	159.7	61.8	0.4848
NB4	15	2	1.9317	1.9765	158.7	63.7	0.4721
KB1	0	2	1.9425	1.9711	158.7	57.1	0.5400
KB2	5	2	1.9385	1.9711	158.8	58.0	0.5198
KB3	10	2	1.9311	1.9705	158.2	61.6	0.5012
KB4	15	2	1.9311	1.9711	158.2	63.5	0.4839

[a] $A_{\|}$ and $A_{\perp}$ are negative.

Table 2
Spin Hamiltonian parameters[a] of VO^{2+} at room temperature and Λth in $xMoO_3{\cdot}(70-x)B_2O_3{\cdot}30M_2O$ (M = Li, Na & K) glasses.

Glass no.	x (mol%)	V_2O_5 (mol%)	$g_{\|\|}$ (±0.0010)	$g_\perp$ (±0.0010)	$\|A_{\|\|}\|$ (10^{-4} cm^{-1}) (±1.0)	$\|A_\perp\|$ (10^{-4} cm^{-1}) (±1.0)	Λth
BL1[b]	0	2	1.9374	1.9720	162.8	58.9	0.4940
BL2	5	2	1.9345	1.9720	162.6	58.9	0.4974
BL3	10	2	1.9317	1.9720	162.3	58.9	0.5008
BL4	15	2	1.9288	1.9720	162.1	58.9	0.5043
BN1[b]	0	2	1.9391	1.9711	160.2	57.1	0.5134
BN2	5	2	1.9377	1.9711	160.1	57.1	0.5168
BN3	10	2	1.9334	1.9696	160.7	57.0	0.5202
BN4	15	2	1.9305	1.9687	160.4	57.0	0.5237
BK1[b]	0	2	1.9425	1.9711	158.7	57.1	0.5400
BK2	5	2	1.9357	1.9664	159.1	56.9	0.5434
BK3	10	2	1.9311	1.9664	159.6	56.9	0.5468
BK4	15	2	1.9268	1.9649	159.7	56.9	0.5503

[a] $A_{\|\|}$ and $A_\perp$ are negative.
[b] Glass Nos. BL1 & LB1, BN1 & NB1 and BK1 & KB1 have same composition.

Table 3
P, K, $|A'_{\|\|}|$, $|A'_\perp|$, $\Delta g_{\|\|}/\Delta g_\perp$, α^2 and γ^2 of VO^{2+} in $xMoO_3{\cdot}(30-x)M_2O{\cdot}70B_2O_3$ (M = Li, Na and K) glasses at room temperature.

Glass no.	P (10^{-4} cm^{-1})	K	$\|A'_{\|\|}\|$ (10^{-4} cm^{-1})	$\|A'_\perp\|$ (10^{-4} cm^{-1})	$\Delta g_{\|\|}/\Delta g_\perp$	α^2	γ^2
LB1	114.0	0.779	74.0	29.9	2.1429	0.589	0.778
LB2	113.5	0.780	74.0	29.6	2.1734	0.615	0.801
LB3	107.2	0.851	70.1	28.5	2.8308	0.648	0.649
LB4	104.4	0.881	68.4	27.8	2.9567	0.661	0.633
NB1	113.5	0.764	73.5	29.6	2.0268	0.567	0.797
NB2	110.9	0.793	72.2	29.0	2.1185	0.599	0.797
NB3	106.7	0.843	69.7	28.2	2.5632	0.635	0.698
NB4	103.5	0.881	67.6	27.5	2.7326	0.640	0.660
KB1	112.2	0.770	72.3	29.3	1.9164	0.533	0.792
KB2	110.9	0.784	71.9	29.0	2.0452	0.569	0.792
KB3	105.3	0.846	69.1	27.5	2.2404	0.635	0.807
KB4	103.3	0.876	67.8	27.0	2.2829	0.635	0.792

Table 4
P, K, $|A'_{\|\|}|$, $|A'_\perp|$, $\Delta g_{\|\|}/\Delta g_\perp$, α^2 and γ^2 of VO^{2+} in $xMoO_3{\cdot}(70-x)B_2O_3{\cdot}30M_2O$ (M = Li, Na and K) glasses at room temperature.

Glass no.	P (10^{-4} cm^{-1})	K	$\|A'_{\|\|}\|$ (10^{-4} cm^{-1})	$\|A'_\perp\|$ (10^{-4} cm^{-1})	$\Delta g_{\|\|}/\Delta g_\perp$	α^2	γ^2
BL1[a]	114.0	0.779	74.0	29.9	2.1429	0.589	0.778
BL2	113.4	0.782	74.0	29.7	2.2371	0.615	0.778
BL3	112.8	0.784	73.9	29.5	2.3310	0.640	0.778
BL4	112.2	0.787	73.8	29.4	2.4247	0.666	0.778
BN1[a]	113.5	0.764	73.5	29.6	2.0268	0.567	0.797
BN2	113.2	0.765	73.5	29.6	2.0727	0.580	0.797
BN3	113.4	0.763	74.2	29.5	2.1099	0.618	0.835
BN4	112.8	0.764	74.2	29.3	2.1389	0.644	0.857
BK1[a]	112.2	0.770	72.3	29.3	1.9164	0.533	0.792
BK2	112.1	0.765	73.3	28.9	1.8557	0.595	0.912
BK3	112.1	0.765	73.8	28.9	1.9826	0.635	0.912
BK4	111.8	0.765	74.1	28.7	2.0183	0.673	0.949

[a] Glass Nos. BL1 & LB1, BN1 & NB1 and BK1 & KB1 have same composition.

increases the positive charge on V^{4+} and increases the π bonding between V^{4+} and vanadyl oxygen. This increase, in turn, decreases the bond length of V^{4+} -(vanadyl oxygen). Consequently, the tetragonal nature of the $V^{4+}O_6$ complex is enhanced. From Table 1, it is observed that the theoretical optical basicity, Λth, of the host glass decreases when M_2O is replaced by MoO_3. This decrease in Λth, predicts that the tetragonal distortion should increase with increase in MoO_3:M_2O ratio, thus the variation in theoretical optical basicity is in agreement with the SHP in $M_2O{\cdot}MoO_3{\cdot}B_2O_3$ glasses.

Tables 2 and 4 show that in $MoO_3{\cdot}B_2O_3{\cdot}Li_2O$ glasses, the values of $g_{\|\|}$, $|A_{\|\|}|$, P, $|A'_{\|\|}|$ and $|A'_\perp|$ decrease whereas the values of K and $\Delta g_{\|\|}/\Delta g_\perp$ increase with increase in the MoO_3 content and hence there is a increase in the tetragonal nature of the $V^{4+}O_6$ complex i.e. the octahedral symmetry is reduced with increase in MoO_3 content. The expansion of the $3d_{xy}$ orbit also observed due to decrease in the value of 'P', which suggests that there is a "screen effect" [32]. Similar kinds of results were already observed in $MoO_3{\cdot}Li_2O{\cdot}B_2O_3$ glasses. Table 2 shows that, Λth increases with increase in MoO_3:B_2O_3 ratio. This variation predicts that the tetragonal distortion should decrease with increase in MoO_3:B_2O_3 ratio which shows that the theoretical optical basicity is independent of SHP.

In $MoO_3{\cdot}B_2O_3{\cdot}Li_2O$ glasses, it is observed that the variation in the values of $|A_{\|\|}|$, $|A_\perp|$, P, $|A'_{\|\|}|$, $|A'_\perp|$and K with increase in MoO_3:B_2O_3 ratio is within experimental error in Tables 2 and 4. The values of $g_{\|\|}$ and $g_\perp$ decrease and that of $\Delta g_{\|\|}/\Delta g_\perp$ increases with increase in MoO_3 content. Small increase in the value of $\Delta g_{\|\|}/\Delta g_\perp$ suggests that the octahedral symmetry of $V^{4+}O_6$ complex is slightly reduced when B_2O_3 is replaced by MoO_3. As the variation in the values of P, $|A'_{\|\|}|$ and $|A'_\perp|$ is within experimental error, therefore the average radius of the unpaired electron in vanadium remains unchanged.

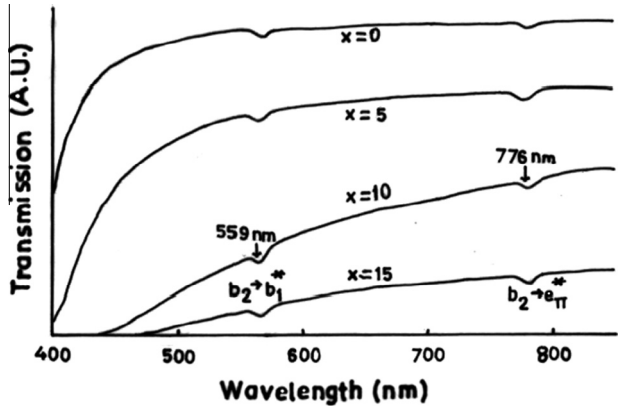

Fig. 3. The optical transmission spectra of xMoO$_3$·$(30-x)$Na$_2$O·70B$_2$O$_3$ glasses doped with 2 mol% of V_2O_5 at 300 K.

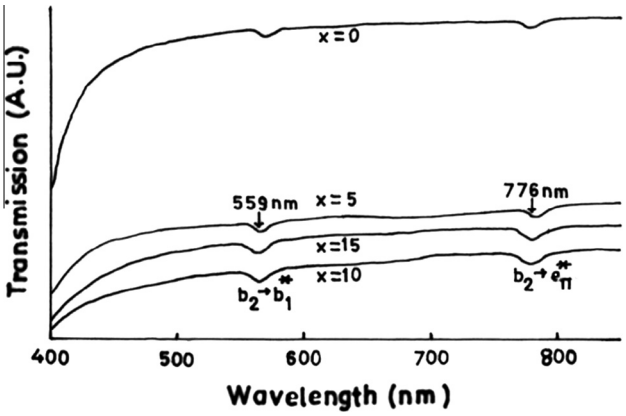

Fig. 4. The optical transmission spectra of xMoO$_3$·$(70-x)$B$_2$O$_3$·30Na$_2$O glasses doped with 2 mol% of V_2O_5 at 300 K.

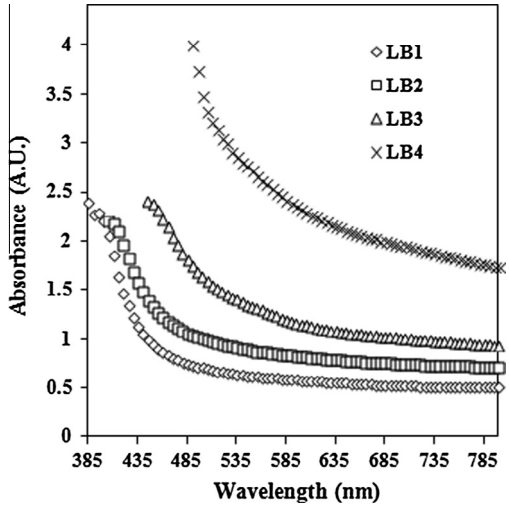

Fig. 5. The optical absorption spectra of xMoO$_3$·$(30-x)$Li$_2$O·70B$_2$O$_3$ glasses.

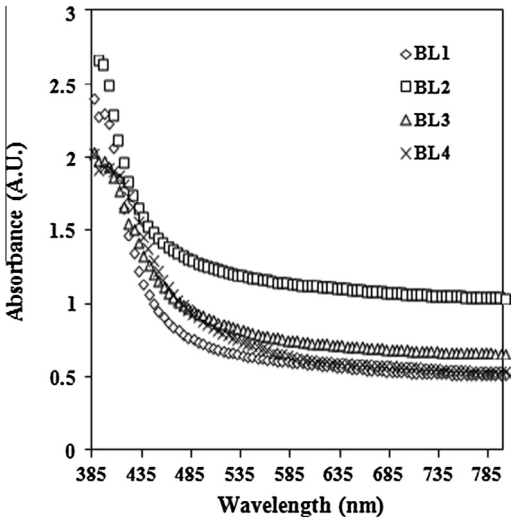

Fig. 6. The optical absorption spectra of xMoO$_3$·$(70-x)$B$_2$O$_3$·30Li$_2$O glasses.

Table 5
Cut off wavelength (λ_{cutoff}), Optical band gap (E_g), B and tailing parameter (B) and Urbach's energy (ΔE) of xMoO$_3$·$(30-x)$M$_2$O·70B$_2$O$_3$ (M = Li, Na and K) glasses doped with 2 mol% of V_2O_5.

Glass no.	x (mol%)	λ_{cutoff} (nm)	E_g (eV)	B (cm eV)$^{-1}$	ΔE (eV)
LB1	0	400	2.54	14.10	0.29
LB2	05	405	2.11	08.44	0.51
LB3	10	445	1.59	06.75	0.66
LB4	15	490	1.37	09.13	0.69
NB1	0	383	2.94	29.40	0.14
NB2	05	390	2.54	14.70	0.32
NB3	10	390	2.55	13.79	0.30
NB4	15	470	1.89	11.76	0.44
KB1	0	365	3.11	49.65	0.13
KB2	5	400	2.03	9.78	0.56
KB3	10	430	1.68	7.24	0.63
KB4	15	475	1.62	9.82	0.59

Table 6
Cut off wavelength (λ_{cutoff}), Optical band gap (E_g), B and tailing parameter (B) and Urbach's energy (ΔE) of xMoO$_3$·$(70-x)$B$_2$O$_3$·30M$_2$O (M = Li, Na and K) glasses doped with 2 mol% of V_2O_5.

Glass no.	x (mol%)	λ_{cutoff} (nm)	E_g (eV)	B (cm eV)$^{-1}$	ΔE (eV)
BL1[a]	0	400	2.54	14.10	0.29
BL2	5	402	2.18	10.33	0.50
BL3	10	405	1.89	7.17	0.55
BL4	15	410	1.72	6.22	0.81
BN1[a]	0	383	2.94	29.40	0.14
BN2	5	385	2.61	14.05	0.26
BN3	10	390	2.55	13.79	0.30
BN4	15	394	2.24	7.89	0.45
BK1[a]	0	365	3.11	49.65	0.13
BK2	5	385	2.70	12.37	0.22
BK3	10	388	2.64	12.02	0.26
BK4	15	393	2.59	14.55	0.29

[a] Glass nos. LB1 & BL1, NB1 & BN1 and KB1 & BK1 have same composition.

Such results are not observed in MoO$_3$·Na$_2$O·B$_2$O$_3$ glasses. Similar kinds of results were already observed in MoO$_3$·Na$_2$O·B$_2$O$_3$ glasses. Table 2 shows that, Ath increases with increase in MoO$_3$:B$_2$O$_3$ ratio. This variation predicts [36,37] that the tetragonal distortion should decrease with increase in MoO$_3$:B$_2$O$_3$ ratio which is independent of variation in SHPs.

In MoO$_3$·B$_2$O$_3$·K$_2$O glasses, Tables 2 and 4 show that the values of $g_{\|}$, $g_{\perp}$, $|A'_{\perp}|$, and $\Delta g_{\|}/\Delta g_{\perp}$ decrease whereas the values of P and K decrease slightly and the variation in the value of $|A_{\perp}|$ is within experimental error. The values of $|A_{\|}|$and $|A'_{\|}|$ increase with increase in MoO$_3$:B$_2$O$_3$ ratio. Decrease in the value of $\Delta g_{\|}/\Delta g_{\perp}$ also shows that the octahedral symmetry of $V^{4+}O_6$ complex is improved

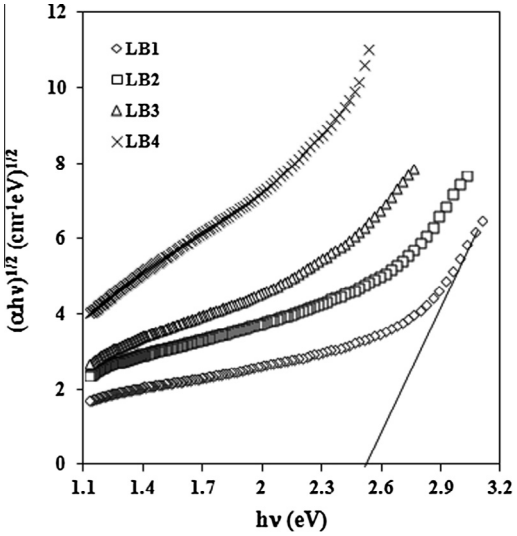

Fig. 7. Tauc's plot for $x MoO_3 \cdot (30 - x)Li_2O \cdot 70B_2O_3$ glasses.

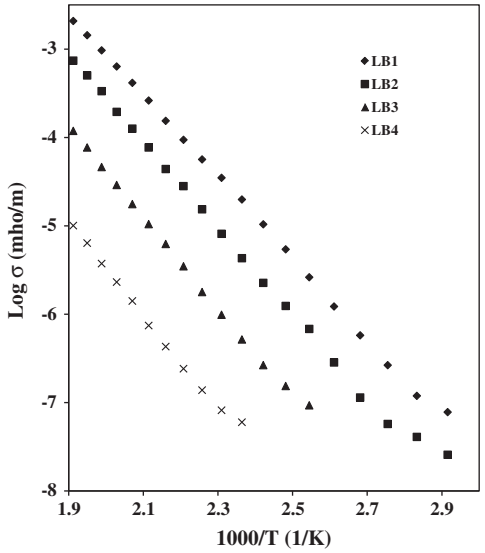

Fig. 9. Variation of Log σ versus $10^3\ T^{-1}$ for $x MoO_3 \cdot (30 - x)Li_2O \cdot 70B_2O_3$ glasses.

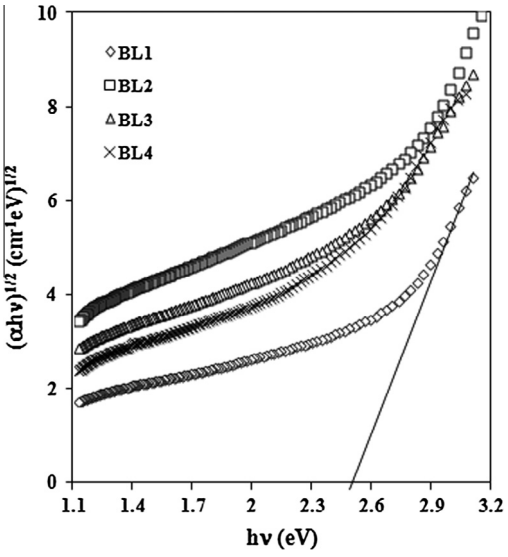

Fig. 8. Tauc's plot for $x MoO_3 \cdot (70 - x)B_2O_3 \cdot 30Li_2O$ glasses.

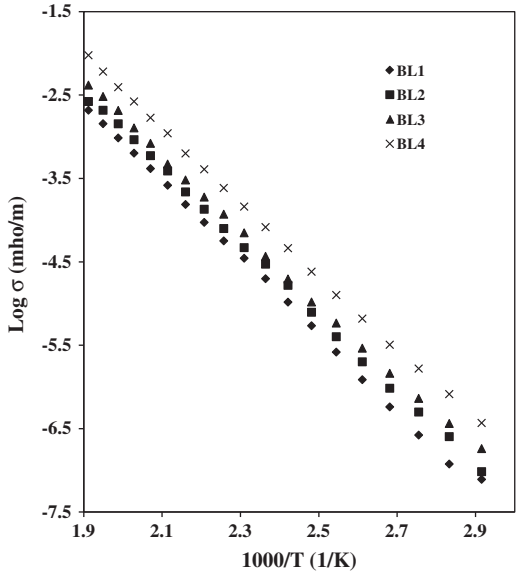

Fig. 10. Variation of Log σ versus $10^3\ T^{-1}$ for $x MoO_3 \cdot (70 - x)B_2O_3 \cdot 30Li_2O$ glasses.

when B_2O_3 is replaced by MoO_3 at constant K_2O. Decrease in the value of P and $|A'_{\perp}|$show that the $3d_{xy}$ orbit expands with increase in mol% of MoO_3 in such glasses and from Table 2 it observed that Λth increases with increase in MoO_3:B_2O_3 ratio. This variation predicts that the tetragonal distortion should decrease with increase in MoO_3:B_2O_3 ratio which shows that the variation in Λth is in agreement with SHPs.

Table 2 shows that, Λth increases with increase in MoO_3:B_2O_3 ratio. This variation predicts that the tetragonal distortion should decrease with increase in MoO_3:B_2O_3 ratio which shows that the theoretical optical basicity is independent of SHP in $MoO_3 \cdot B_2O_3 \cdot M_2O$ glasses.

4.2. Optical spectra

In the present study, only two transmission bands are observed for all the glasses. Figs. 3 and 4 show the optical transmission spectra of $x MoO_3 \cdot (30 - x)Na_2O \cdot 70B_2O_3$ and $x MoO_3 \cdot (70 - x)B_2O_3 \cdot 30Na_2O$ glass samples. Similar spectra were observed for other samples. The positions of the two transmission bands are also shown in these figures. It is observed that within the same glass system, there is no change in the positions of the two bands with increase in MoO_3 content. These two bands are typical for VO^{2+} and can be assigned to $b_2 \rightarrow b_1^*$ and $b_2 \rightarrow e_\pi^*$ transitions, respectively. The values of $g_{||}$ and $g_\perp$ are related to bonding parameters [32]. The expressions $(1 - \alpha^2)$ and $(1 - \gamma^2)$ are the covalency rates. The values of α^2 and γ^2 were calculated and are given in Tables 3 and 4. These tables show that the value of α^2 increases with increase in MoO_3:M_2O and MoO_3:B_2O_3 ratio, which indicates that the degree of covalency of the σ-bonding decreases in these glasses. It is also observed from Tables 3 and 4, that the value of γ^2 decreases with increase in MoO_3:-Li_2O or MoO_3:Li_2O ratio, which indicates that the degree of covalency of the π-bonding increases. Tables 3 and 4 show that the value of γ^2 remains unchanged with increase in MoO_3 content, which indicates that there is no change in the degree of covalency of the π-bonding. Tables 3 and 4 show that the value of γ^2 increases with increase in MoO_3:B_2O_3 ratio (keeping Na_2O and K_2O constant), thereby indicating that the degree of covalency of the π-bonding de-

Table 7
DC conductivity (σ), Log σ_0 and activation energy (W) of $x$$MoO_3$·(30 − x) M_2O·70B_2O_3 (M = Li, Na & K) glasses.

Glass no.	x (mol%)	V_2O_5 (mol%)	σ_{at423K} (Ω^{-1} m^{-1})	σ_{at523K} (Ω^{-1} m^{-1})	Log σ_0 (Ω^{-1} m^{-1})	W (eV)
LB1	0	2	1.99×10^{-5}	2.08×10^{-3}	6.06	0.91
LB2	5	2	4.30×10^{-6}	7.40×10^{-4}	5.78	0.93
LB3	10	2	5.18×10^{-7}	1.19×10^{-4}	5.69	1.00
LB4	15	2	5.99×10^{-8}	1.01×10^{-5}	4.75	1.02
NB1	0	2	2.02×10^{-5}	4.68×10^{-4}	5.49	0.91
NB2	5	2	1.09×10^{-5}	2.13×10^{-4}	5.36	0.93
NB3	10	2	5.10×10^{-7}	1.66×10^{-5}	4.51	0.97
NB4	15	2	9.65×10^{-8}	2.79×10^{-6}	4.04	1.00
KB1	0	2	1.60×10^{-5}	1.38×10^{-4}	5.17	0.94
KB2	5	2	4.51×10^{-6}	5.42×10^{-5}	4.93	0.96
KB3	10	2	2.75×10^{-7}	3.07×10^{-6}	4.54	1.04
KB4	15	2	2.29×10^{-8}	2.75×10^{-7}	3.74	1.07

Table 8
DC conductivity (σ), Log σ_0 and activation energy (W) of $x$$MoO_3$·(70 − x) B_2O_3·30M_2O (M = Li, Na & K) glasses.

Glass no.	x (mol%)	V_2O_5 (mol%)	σ_{at343K} (Ω^{-1} m^{-1})	σ_{at523K} (Ω^{-1} m^{-1})	Log σ_0 (Ω^{-1} m^{-1})	W (eV)
BL1[a]	0	2	7.80×10^{-8}	2.08×10^{-3}	6.06	0.91
BL2	5	2	9.65×10^{-8}	2.65×10^{-3}	6.03	0.89
BL3	10	2	1.82×10^{-7}	4.16×10^{-3}	6.08	0.88
BL4	15	2	3.70×10^{-7}	9.49×10^{-3}	6.34	0.87
BN1[a]	0	2	6.91×10^{-8}	4.68×10^{-4}	5.49	0.91
BN2	5	2	1.78×10^{-7}	7.93×10^{-4}	5.33	0.88
BN3	10	2	2.52×10^{-7}	1.03×10^{-3}	5.42	0.87
BN4	15	2	3.08×10^{-7}	1.30×10^{-3}	5.39	0.86
BK1[a]	0	2	4.22×10^{-8}	1.38×10^{-4}	5.17	0.94
BK2	5	2	5.89×10^{-8}	1.86×10^{-4}	5.24	0.93
BK3	10	2	8.76×10^{-8}	2.64×10^{-4}	5.23	0.91
BK4	15	2	1.38×10^{-7}	3.08×10^{-4}	4.90	0.87

[a] Glass nos. LB1 & BL1, NB1 & BN1 and KB1 & BK1 have same composition.

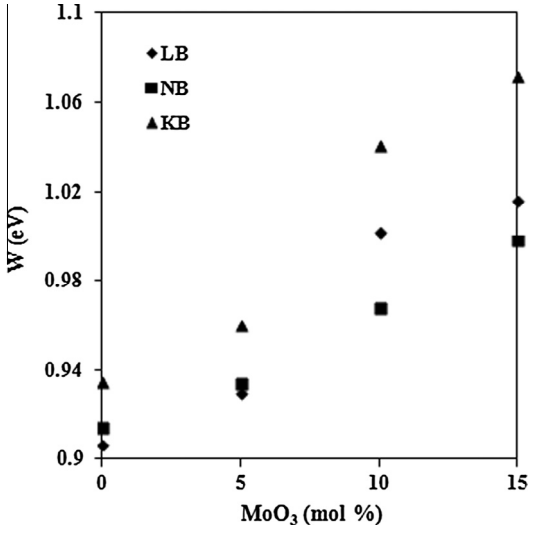

Fig. 11. Variation of activation energy, W with mol% of MoO_3 in $x$$MoO_3$·(30 − x)M_2O·70B_2O_3 glasses.

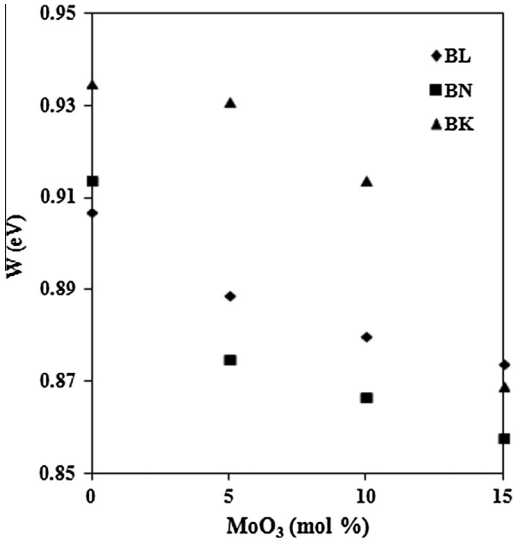

Fig. 12. Variation of activation energy, W with mol% of MoO_3 in $x$$MoO_3$·(70 − x)B_2O_3·30M_2O glasses.

creases. These findings based on optical transmission are in agreement with the EPR results.

Tables 5 and 6 show that value of λ_{cutoff} increases with increase in MoO_3 content. The shift in λ_{cutoff} is about 10–30 nm with increase MoO_3:B_2O_3 ratio at constant M_2O, whereas this shift is about 100 nm with increase in MoO_3:M_2O ratio at constant B_2O_3. Therefore it appears that MoO_3 plays different roles in these two glass systems.

According to the theory of electronic structure of amorphous material [38], the optical absorption edge in the materials at higher levels of absorption coefficient is interpreted in terms of indirect transitions. It is observed from Tables 5 and 6 that the value of E_g decreases with increase in MoO_3 content in the glass samples and its values lie between 3.11 eV and 1.37 eV. This decrease in E_g may be associated with the increase in the formation of non-bridging oxygens [39–41]. Further, the rate of decrease in E_g is much faster for the glass systems in which MoO_3 replaces B_2O_3 in comparison to the glass systems in which it replaces M_2O. This may be possibly because of the formation of larger number of

nonbridging oxygens in the former case in comparison to the latter case.

The values of the band tailing parameter, B lies between 49.65 to 6.22 $(cm\ eV)^{-1}$. These values are in agreement with the reported values for inorganic glasses [42]. It has been observed that for most materials the width of absorption tail (just below the conduction band), ΔE, ranges from 0.006 to 0.014 eV which is a broad range to draw any conclusive remark about any specific mechanism of absorption edge operative in a particular material. However, it is generally assumed [43] that the exponential tail observed in various materials and in their different structures must have the same physical origin. This origin may be attributed to the phonon-assisted indirect electronic transitions. In the present glass systems, the ΔE values vary from 0.22 to 0.81 eV and these values are in agreement with the reported values [44] for inorganic glasses.

4.3. dc conductivity

4.3.1. $xMoO_3{\cdot}(30-x)M_2O{\cdot}70B_2O_3$ (M = Li, Na and K) glasses

The ionic conductivity of oxide glasses can be expressed by equation suggested by [45]. In the present glass systems, the total density of alkali ion is known but the fraction of these, which are mobile and contribute to the measured conductivity, is unknown. In ionically conducting glasses, both the concentration and mobility of ions are dependent on the composition and structure. In molybdenum containing glasses, both Mo^{6+} and Mo^{5+} valence states are found to coexist [28,29]. Therefore it is expected that the dc conductivity may also have contribution in the form of electronic conductivity due to electron hopping from the lower valence state, Mo^{5+} (donor level), to the higher valence state, Mo^{6+} (acceptor level), which is in accordance with the mechanism of conduction proposed in other transition metal oxide glasses [8,45–47] and interaction between the electrons and lattice is sufficiently strong to produce a small polaron [7,8]. However in the present glass systems conductivity decreases with increase in MoO_3:M_2O ratio, therefore it appears that there is a competition between ionic and electronic conductivity and rate of decrease in the former is faster than the rate of increase in the latter. Similar results have been reported by El-Desoky [48] and Jayasinghe [49,50] et al for the conductivity studies of M_2O–V_2O_5–TeO_2 (M = Li, Na, K) glasses. The values of activation energy presented in Table 5 supports the argument that ionic conduction is occurring in these glasses.

4.3.2. $xMoO_3{\cdot}(70-x)B_2O_3{\cdot}30M_2O$ (M = Li, Na and K) glasses

In the present glass systems the increase in dc conductivity with increase in MoO_3:B_2O_3 ratio, at constant M_2O content (30 mol%), is possibly due to the increasing contribution of the electronic conductivity. The dc electronic conductivity in the glasses containing transition metal ions is expressed as [4,5]:

$$S = (v_0 Ne^2R^2/kT)C(1-C)\exp(-2\alpha R)\exp(-W/kT)$$

where v_0 is the jump frequency, N is the number of sites of TM ions per unit volume, e is the electronic charge, R is the average distance between two sites, C is the fraction of sites in the low valence states, α is the tunneling probability and W is the activation energy for the conduction process. For $x = 0$, the conductivity is purely ionic in nature, however, for $x > 0$, the electrical conductivity is also having electronic contribution. Doweidar [51] et al observed that in Na_2O–V_2O_5–B_2O_3 glasses the conductivity increased with increase in V_2O_5:B_2O_3 ratio at constant Na_2O and they attributed this behavior because of the electronic conduction. Similarly, Chowdari et al. [52] et al reported that in lithium molybdophosphate glasses at constant Li_2O content, the dc conductivity increases with MoO_3 content. Therefore, the present glass systems are mixed ionic-electronic conductors.

5. Conclusions

V^{4+} ions in these samples exist as VO^{2+} ions in octahedral coordination with a tetragonal compression and belong to C_{4V} symmetry. There is an increase in the tetragonal nature of $V^{4+}O_6$ complex with increase in MoO_3 content in $MoO_3{\cdot}Li_2O{\cdot}B_2O_3$ and $MoO_3{\cdot}Na_2O{\cdot}B_2O_3$ glasses; and in these glasses octahedral symmetry of $V^{4+}O_6$ is reduced. The tetragonal nature of $V^{4+}O_6$ complex decreases and the octahedral symmetry is improved with increase in MoO_3:B_2O_3 ratio keeping K_2O content constant whereas tetragonality of $V^{4+}O_6$ complex increases with increase in MoO_3:K_2O ratio keeping B_2O_3 constant. Variation in theoretical optical basicity, Λth is in agreement with the SHPs in LB, NB, KB and BK glass series whereas it is independent of SHPs in case of BL and BN glass series. The $3d_{xy}$ orbit of unpaired electron in the VO^{2+} ion expands with increase in MoO_3 content in all the glasses. By the study of optical transmission spectra it is observed that for all the glasses the degree of covalency of the σ-bonding decreases with increase in MoO_3 content and the degree of covalency of the π-bonding also varies. These results based on optical spectroscopy are in agreement with EPR findings. The optical band gap decreases with increasing MoO_3 content in all the glasses because of increase in the concentration of non-bridging oxygens. The dc conductivity decreases and activation energy increases with increase in MoO_3:M_2O (M = Li, Na, K) ratio in $xMoO_3{\cdot}(30-x)M_2O{\cdot}70B_2O_3$ glasses, whereas the conductivity increases and activation energy decreases with increase in MoO_3:B_2O_3 ratio in $xMoO_3{\cdot}(70-x)\ B_2O_3{\cdot}30M_2O$ glasses.

Acknowledgements

The authors are thankful to UGC, New Delhi for providing the financial and experimental support under the Major Research Project.

References

[1] O. Cozar, D.A. Magdas, I. Ardelean, J. Non-Cryst. Solids 354 (2008) 1032.
[2] N.S. Vedeanu, D.A. Magdas, J. Alloys Compds. 534 (2012) 96.
[3] B. Sreedhar, M. Sairam, D.K. Chattopadhyay, K. Kojima, Mater. Chem. Phys. 92 (2005) 492.
[4] M. Shaaban, E.A. Salem, E. Mohamed, J. Non-Cryst. Solids 357 (2011) 1153.
[5] S. Khasa, R.M. Krishna, J.J. Andre, V.P. Seth, S.K. Gupta, Mater. Res. Bull. 34 (1999) 1089.
[6] M. Abo-Naf Sherief, J. Non-Cryst. Solids 358 (2012) 406.
[7] A. Mansingh, J.K. Vaid, R.P. Tandon, J. Phys. C: Solid State Phys. 10 (1977) 4061.
[8] M.H. Hekmat-Shoar, C.A. Hogarth, G.R. Moridi, J. Mater. Sci. 20 (1985) 889.
[9] S. Sanjay, N. Kishore, A. Agarwal, J. Alloys Compds. 487 (2009) 52.
[10] S. Sanjay, N. Kishore, A. Agarwal, Ind. J. Pure Appl. Phys. 46 (2008) 719.
[11] B. Bridge, N.D. Patel, J. Non-Cryst. Solids 91 (1987) 27.
[12] E. Mansour, G.M. El-Damrawi, Y.M. Moustafa, S.A. El-Maksoud, H. Doweidar, Physica B 293 (2001) 268.
[13] S. Khasa, V.P. Seth, P.S. Gahlot, A. Agarwal, R.M. Krishna, S.K. Gupta, Physica B 334 (2003) 347.
[14] H.G. Hecht, T.S. Johnston, J. Chem. Phys. 46 (1967) 23.
[15] B. Bleaney, K.D. Bowers, M.H. Pryce, Proc. R. Soc. (London) A228 (1955) 147.
[16] S. Khasa, V.P. Seth, A. Agarwal, R.M. Krishna, S.K. Gupta, P. Chand, Mater. Chem. Phys. 72 (2001) 366.
[17] G. Hochstrasser, Phys. Chem. Glasses 7 (1966) 178.
[18] H. Toyuki, S. Akagi, Phys. Chem. Glasses 15 (1974) 1.
[19] A.M. Abdelghany, H.A. ElBatal, J. Mol. Struct. 1024 (2012) 47.
[20] A. Agarwal, V.P. Seth, P.S. Gahlot, S. Khasa, P. Chand, J. Phys. Chem. Solids 64 (2003) 2281.
[21] T. Suzuki, M. Hirano, H. Hosono, J. Appl. Phys. 91 (2002) 4149.
[22] C. Dayanand, G. Bhikshamaiah, M. Salagram, Mater. Lett. 23 (1995) 69.
[23] M. Chaudhary, M. Altaf, Mater. Lett. 34 (1998) 213.
[24] M. Salagram, V.K. Prasad, K. Subrahmanyam, Opt. Mater. 18 (2002) 367.
[25] R.P.S. Chakradhar, K.P. Ramesh, J.L. Rao, J. Ramakrishna, J. Phys.: Cond. Matter 15 (2003) 1469.
[26] P. Roychoudhary, S.K. Batabyal, A. Paul, C. Basu, S. Mukherjee, K. Goswami, J. Appl. Phys. 92 (2002) 3530.
[27] Y. Watanabe, S. Sakata, T. Watanabe, T. Tsuchiya, J. Non-Cryst. Solids 240 (1998) 212.
[28] M. Pal, K. Hirota, Y. Tsujigami, H. Sakata, J. Phys. D: Appl. Phys. 34 (2001) 459.
[29] N.M. Bobkova, I.L. Rakov, N.P. Solovei, J. Non-Cryst. Solids 111 (1989) 98.
[30] D. Kivelson, S. Lee, J. Chem. Phys. 41 (1964) 1896.

[31] B.R. Mcgarvey, in: R.L. Carlin (Ed.), Transition Metal Chemistry, vol. 3, Dekker NY, p. 115.
[32] A.K. Bandopadhayay, J. Mater. Sci. 16 (1981) 189.
[33] H. Hosono, H. Kawazoe, T. Kanazawa, J. Non-Cryst. Solids 37 (1980) 427.
[34] I. Ardelean, O. Cozar, Gh. Ilonca, J. Non-Cryst. Solids 68 (1984) 33.
[35] V.P. Seth, A. Yadav, Phys. Chem. Glasses 28 (1986) 109.
[36] A. Klonkowski, Phys. Chem. Glasses 26 (1985) 11.
[37] H. Hosono, H. Kawazoe, T. Kanazawa, J. Non-Cryst. Solids 33 (1974) 125.
[38] E.A. Davis, N.F. Mott, Phil. Mag. 22 (1970) 903.
[39] K. Terashima, S.H. Kim, T. Yoko, J. Am. Ceram. Soc. 78 (1995) 1601.
[40] R.N. Sheibani, C.A. Hogarth, J. Mater. Sc. 26 (1991) 429.
[41] C. Dayanand, R.V.G.K. Sarma, G. Bhikshamaiah, M. Salagram, J. Non-Cryst. Solids 167 (1994) 122.
[42] Y.C. Ratnakaram, A.V. Reddy, J. Non-Cryst. Solids 277 (2000) 142.
[43] K.L. Chopra, S.K. Bahl, Thin Solid Films 11 (1972) 377.
[44] A.M. Glass, K. Nassau, J. Appl. Phys. 51 (1980) 3756.
[45] J.C. Bazan, J.A. Duffy, M.D. Ingram, M.R. Mallace, Solid State Ionics 86–88 (1996) 497.
[46] G.F. Lynch, M. Sayer, S.L. Segel, G. Rosenblatt, J. Appl. Phys. 42 (1970) 2587.
[47] P. Huang, X. Huang, F. Gan, Solid State Ionics 44 (1990) 11.
[48] M.M. El-Desoky, Mater. Chem. Phys. 73 (2002) 259.
[49] G.D.L.K. Jayasinghe, M.A.K.L. Dissanayake, M.A. Careem, J.L. Souquet, Solid State Ionics 93 (1997) 291.
[50] G.D.L.K. Jayasinghe, M.A.K.L. Dissanayake, P.W.S.K. Bandaranayake, R.P. Gunawardane, Solid State Ionics 78 (1995) 199.
[51] H. Doweidar, A. Megahed, I.A. Gohar, J. Phys. D: Appl. Phys. 19 (1986) 1939.
[52] B.V.R. Chowdari, K.L. Tan, W.T. Chia, R. Gopalakrishnan, J. Non-Cryst. Solids 128 (1991) 18.